XXXVI Ibero-Latin American Congress on Computational Methods in Engineering
CILAMCE
Rio de Janeiro, 22-25 Nov 2015

MONTE CARLO SIMULATION TO PREDICT FATIGUE SN CURVE IN ALUMINUM FRICTION STIR WELDS

Antonio Carlos de Oliveira Miranda

Scott Walbridge

acmiranda@unb.br

swalbrid@uwaterloo.ca

Department of Civil and Environmental Engineering, University of Brasília, SG-12 Building, Darcy Ribeiro Campus, 70.910-900, Brasilia, DF, Brazil

Department of Civil and Environmental Engineering, University of Waterloo, 200 University Ave. West, N2L 3G1, Waterloo, Ontario, Canada,

Abstract. *Recent papers on the fatigue design of aluminum welds have highlighted a lack of guidance in existing codes and standards for the fatigue assessment of aluminum alloy structures containing joints made by friction stir welding (FSW). Structural design code writers in North America and Europe are starting to address this need. In addition to provisions on fatigue performance, codes and standards are also beginning to appear that provide guidance on welding procedures and quality control. However, these provisions seem to be prescriptive from the point of view of fatigue, and the influence of defects resulting from the welding process on the fatigue performance have not been extensively studied. Against this background, the goals of the current paper are: 1) to perform a statistical analysis of available fatigue life data for FSW joints and compare the results to design stress-life (S-N) curves in various codes and standards using Monte Carlo approach; 2) to present a review of the literature on FSW joints with a focus on the material and geometric parameters required to perform a fracture mechanics analysis of these joints; and 3) to show how probabilistic fracture mechanics, given these parameters, can aid in establishing and refining the quality control guidelines for cyclically loaded FSW joints. Based on the presented analysis, parameters are identified for which additional data collection would be beneficial for improving our understanding of the fatigue behavior of FSW joints and how this behavior is affected by the weld quality.*

Keywords: *Aluminum friction stir weld, Fatigue parameter data, Probabilistic analysis*

1 INTRODUCTION

Considering the development of arc welding, the invention and development of friction stir welding (FSW) has been comparatively recent. This welding method was first applied by The Welding Institute (TWI) of UK to aluminum alloys as a solid-state joining technique in 1991. Many studies on FSW have been published since the first stages of development, and many researchers have reported on the advantages and disadvantages of this welding process (Mishra and Ma 2005). Recent papers on the fatigue design of aluminum welds ,e.g. (Maddox 2003), have highlighted a lack of guidance in the existing codes and standards for the fatigue assessment of aluminum alloy structures containing joints made by FSW, in contrast with arc welding.

Structural design code writers in North America and Europe are starting to address this need, based on the available test data and in some cases making assumptions regarding the relationship between the fatigue performance of FSW joints and the existing design curves for similar arc-welded joints. In addition to provisions on fatigue performance, codes are also beginning to appear that provide guidance on welding procedures and quality control (Standardization 2011), design of weld joints, along with qualification of welding operators and procedures (ISO 25239, parts 1-5 (Standardization 2011)). However, these provisions seem to be prescriptive from the point of view of fatigue, and do not consider the role of cyclic loading on imperfections that may occur in the weld. For example, the presence of cavities with a maximum width of 20% of the thickness of the weld, or 4 mm, whichever is less is permitted in ISO 25239 part 5, page 8 (Standardization 2011), although most design specifications will preclude the presence of such imperfections. It is clear that the influence of defects resulting from the welding process on the fatigue performance have not been extensively studied.

Against this background, the goals of the current paper are: 1) to perform a statistical analysis of available fatigue life data for FSW joints and compare the results to design stress-life (S-N) curves in various codes and standards; 2) to present a review of the literature on FSW joints with a focus on the material and geometric parameters required to perform a fracture mechanics analysis of these joints; and 3) to show how probabilistic fracture mechanics, given these parameters, can aid in establishing and refining the quality control guidelines for cyclically loaded FSW joints.

2 BACKGROUND

In friction stir welding, a rotating cylindrical tool with a short protrusion is plunged into two sheets to be joined, and the combination of frictional and deformation heating leads to the consolidation of the two materials when the tool is traversed along the joining line. The final structure in a typical FSW joint is quite different from an arc weld, in that there is typically a fine recrystallized structure consisting of grains usually < 10 µm in size, which is surrounded by thermo-mechanically affected grains closer to the base metal. Due to the deformation caused by the tool, a slightly concave impression is left along the top of the joint, as well as a limited amount of material is ejected and considered ‘flash’ on the top surface. These features may sometimes be considered as inherent flaws by some researchers from the perspective of fatigue analysis, and many fatigue studies of FSW joint performance consider only the weld material below the surface by machining the top and bottom surfaces of the joint completely flat. However, it should be noted that all arc welds also have a comparable weld toe, which presents a similar discontinuity on the surface.

Mishra and Ma (Mishra and Ma 2005) provide an overall review of research on FSW, including some studies on the behaviour of FSW joints performed prior to 2005. They cited the following important observations: (1) the fatigue resistance of FSW specimens in air, in particular the fatigue strength of the FSW joints at 10^7 cycles, was lower than that of the base metal; (2) the surface quality of the FSW joints exerted a significant effect on the fatigue strength of the welds; (3) the effect of the welding parameters on the fatigue strength is complicated with no obvious correlations; and (4) low plasticity burnishing (LPB) after FSW can enhance the fatigue life of FSW joints. Other authors have conducted reviews on other specific aspects of FSW. Ma (Ma 2008) focused on the microstructural aspects of FSW. Nandan et al. (Nandan, DebRoy et al. 2008) reviewed FSW with a focus on heat generation, heat transfer, plastic flow during welding, and elements of tool design to understand the defect formation, structure, and properties of the welded materials. Shtrikman (Shtrikman 2008) and Rai et al. (Rai, De et al. 2011) reviewed the improvement of the welding tools and methods. Murr (Murr 2010) focused in dissimilar metal and alloy systems in order to gain a better understanding of the material flow during FSW, and noted that exceptionally high strain rates and a high degree of material mixing occurs during FSW. Biro et al. (Biro, Chenelle et al. 2012) also reviewed some aspects in microstructure, strength, and crack propagation properties in FSW joints. Numerical modelling and analysis have also been reviewed (Neto and Neto 2013, Hattel, Sonne et al. 2014, He, Gu et al. 2014), however modelling of the fatigue performance coupled with the numerical modeling has not been considered.

3 FATIGUE DATA FOR FSW JOINTS

Design codes for cyclically loaded aluminum structures (e.g. (Hobbacher 2007, Standardization 2007, Association 2010)) generally employ a nominal stress (S-N) approach for fatigue design, wherein the design curve is established based on a statistical analysis of test data, corresponding with a high survival probability (95% or 97.7% – i.e. two standard deviations below the mean – are commonly used). The IIW recommendation (Hobbacher 2007) provides guidelines on how to perform such an analysis to establish these curves. In this section, the available test data is summarized and survival probability curves are established using this approach. These curves are then compared with the design curves from several sources.

Fatigue test results were obtained from 50xx and 60xx aluminum alloys for load ratios ($R = P_{min} / P_{max}$) of 0.1 and -1.0, totaling 226 and 96 points respectively. These alloys were the focus of the study, due to their extensive use in structural applications such as buildings and bridges. Points were digitalized from the following sources: (Okura, Hagisawa et al. 2003) (James, Hattingh et al. 2003) (Dickerson and Przydatek 2003) (Ericsson and Sandström 2003) (Czechowski 2005) (James, Bradley et al. 2005) (Uzun, Dalle Donne et al. 2005) (Zhou, Yang et al. 2005) (Uematsu, Tokaji et al. 2006) (Cavaliere, Campanile et al. 2006) (Zhou, Yang et al. 2006) (Zhou, Yang et al. 2006) (Kobayashi, Sakuma et al. 2007) (Ericsson, Jin et al. 2007) (Moreira, de Figueiredo et al. 2007) (Cavaliere, Squillace et al. 2008) (Kainuma, Katsuki et al. 2008) (Hagisawa and Okura 2009) (Cavaliere, De Santis et al. 2009) (Uematsu, Tokaji et al. 2009) (Grujicic, Arakere et al. 2011) (Sano, Masaki et al. 2012) (Mahdavi Shahri, Höglund et al. 2012) (Vigh and Okura 2013) (Das, Chakraborty et al. 2014) (Vidal, Infante et al. 2014). Results from these sources reported in terms of stress amplitude were converted to stress range ($\Delta S = S_{max} - S_{min}$) where appropriate. Prior to performing the statistical analysis of the data, some of the data points were removed. Specifically, Das et al. (Das, Chakraborty et al. 2014) and Scialpi et al. (Scialpi, De Giorgi et al. 2008) made fatigue tests on specimens with thicknesses of 2 mm and 0.8 mm, respectively. These thicknesses were on the low end of the range and thought to be below the thickness range likely to be used in structural applications. The results obtained by Mahdavi et al. (Mahdavi Shahri, Höglund et al. 2012) and Vigh and Okura (Vigh and Okura 2013) were obtained in deck panels, so they did not follow the standard test in uniaxial tension specimens. The results presented by Dickerson and Przydatek (Dickerson and Przydatek 2003) were obtained with pre-selected 4-7 mm weld root defects. These data points were removed on the basis that such defects would likely be detected and rejected by any adopted quality control procedure. The results obtained by Okura and Hagisawa (Okura, Hagisawa et al. 2003, Hagisawa and Okura 2009) were not included on the basis that they were on the high side of the test data and obtained from an uncommon alloy A6N01S-T5, (specified in JIS H 4100), which is similar (Matsuoka and Kitamura 1999) to the more well-known A6005A alloy, but has different mechanical properties. Also, the results from Czechowsk (Czechowski 2005) and Uematsu et al. (Uematsu, Tokaji et al. 2009) were not included because they polished the specimen surfaces, which would lead to exaggerated fatigue life. The resulting data set contained 155 and 47 results for R = 0.1 and -1.0 respectively. Figure 1 presents the S-N data for the two load ratios. Superimposed on the data are design S-N curves corresponding with 50% and 95% survival probabilities, calculated using the IIW statistical analysis procedure (Hobbacher 2007).

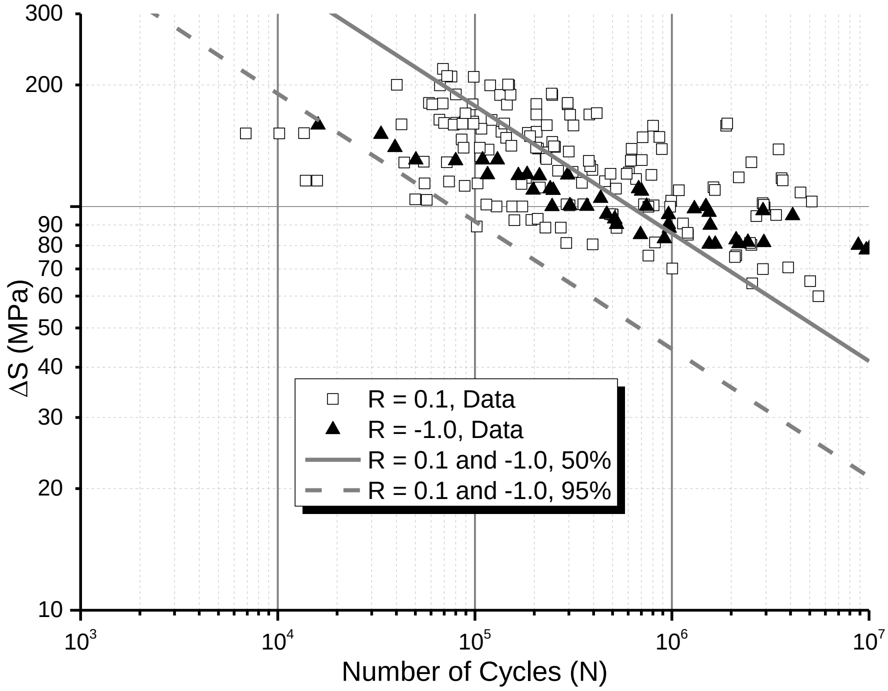

Figure 1. Comparison of data for R = 0.1 and -1.0.

The test data in Fig. 1 includes test results on axially loaded weld specimens, with plate thicknesses ranging from 4.0 to 15.0 mm. The data includes tests on joints made from the following alloys: 5056, 5083, 6005, 6061, 6056, and 6082. The nominal yield strengths of these alloys in their various tempers (varying from annealed to peak aged) ranged from 80.0 to 230 MPa. It can be noted from Fig. 1 that the load ratio, R, has little effect on the S-N data. The flatter slope and reduced scatter in the R = -1 data is thought to be largely the result of the reduced size of the data set. Due to this effect, data sets with different ratios were treated equally to obtain a unique designed curve. The slope (m) of the design S-N curve is m = 3.16. The stress range (ΔS) associated with 2 million cycles is 69.0 MPa, for 50% survival probability, and 35.6 MPa, for 95% survival probability.

Jaccard et al. (Jaccard, Kosteas et al. 1995) recommended a design curve with m = 7 and ΔS ($2{\cdot}10^6$) = 45 MPa for conventional transverse butt weld for aluminum. Figure 2 compares data points of FSW and its design curves with fixed exponent m = 7.0 for 95% survival probability, and the design curve proposed by Jaccard et al. (Jaccard, Kosteas et al. 1995). Note that, for m = 7.0, the stress range in N = $2{\cdot}10^6$ increases 77% compared to the fit design curve m = 3.16, and it is still with 95% of survival probability. In addition, the design curve for FSW presents a high stress level, considering the same exponent m = 7.0, when compared with design curve for conventional one proposed by Jaccard et al. (Jaccard, Kosteas et al. 1995). With this slope, the 95% survival probability curve crosses 2 million cycles at 62 MPa, which translates to a fatigue strength increase of 38%. Comparing the lives associated with a given stress range, this translates to an increase of roughly an order of magnitude. Therefore, using the design curve of a conventional weld in FSW may be considered too conservative.

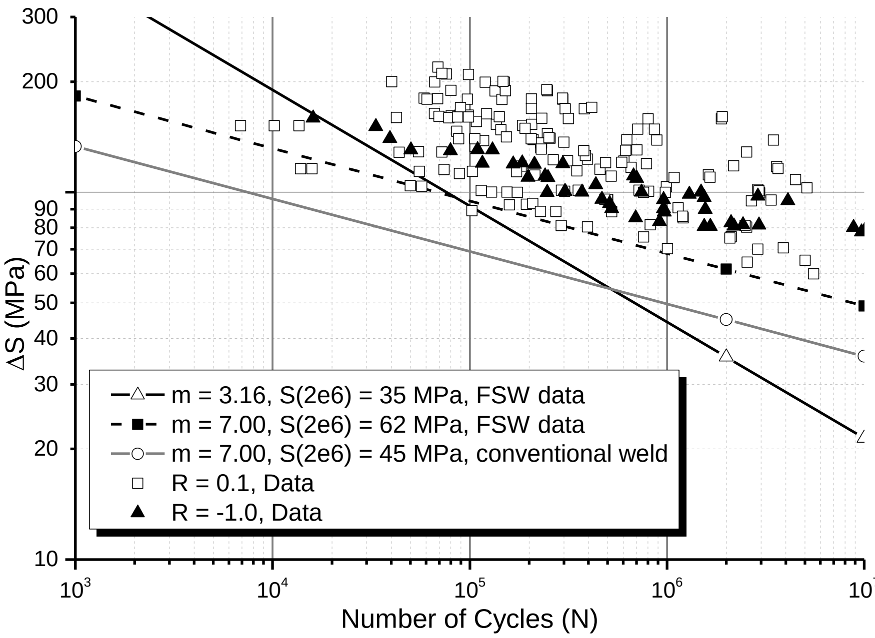

Figure 2. Comparison of test data with different curve slope, *m*

4 DETERMINISTIC FRACTURE MECHANICS MODEL

Following the fatigue life data review, a deterministic fracture mechanics analysis was carried out to determine whether or not the test results could be predicted analytically. A range of deterministic models are available for the fatigue analysis of welded details, with varying levels of accuracy and complexity. Maddox (Maddox 2003) summarizes four methods for assessing the fatigue lives of welded joints, based on the IIW recommendations (Hobbacher 2007). The fracture mechanics approach is one of these methods. In this approach, fatigue crack growth is calculated based on the stress intensity factor (SIF) and associated crack growth rate for the material of interest.

The SIF depends on the crack shape and size. Analytical SIF expressions are available for several 2D crack shapes. For cracks with ellipsoidal fronts in a plate of width W or $2\cdot W$ and thickness t, the SIF range (ΔK) is function of ΔS, a, a/c, a/t, c/W and θ (Newman Jr 1979, Raju and Newman 1988, Anderson 1994), where a and c are the ellipsis semi-axes.

The 2D ellipsoidal crack propagation problem is a reasonable approximation for many actual surface, corner, and internal cracks. Fractographic observations indicate that the successive fronts of those cracks tend to achieve an elliptical form, and to stay approximately elliptic during their fatigue propagation, even when the initial crack shape is far from an ellipsis (De Castro, Giassone et al. 1998). Therefore, it can be quite reasonable to assume in the modelling that the fatigue propagation just changes the shape of the 2D crack (given by the ratio a/c between the ellipsis semi-axes, which quantifies how elongated the cracks are), but preserves their basic ellipsoidal geometry.

As an ellipsis is completely defined by its two semi-axes, to predict the growth of 2D (elliptical) cracks, including their shape changes, it is enough to calculate at each load cycle the lengths of the ellipsis axes a and c, jointly solving the da/dN and the dc/dN propagation problems, where N is the number of cycles applied.

The calculation model requires the crack type and initial size a_i and c_i, the bar geometry, the loading type, the mechanical properties, and the crack propagation rule $da/dN = F(\Delta K, R, \Delta K_{th}, K_c \ldots)$ of the material, where ΔK_{th} and K_c are the threshold SIF range and critical SIF, respectively. A small crack increment δa must also be specified (50 μm, a number of the order of the resolution threshold of the crack measurement methods in fatigue tests, can be a good choice both from the physical and from the numeric points of view). From the loading, ΔS is calculated to obtain:

$$\Delta K\,(a_0) = \Delta S\cdot[\sqrt{(\pi a_i)}\cdot f_a(a_i/c_i,\ a_i/t,\ c_i/W)] \tag{1}$$

The number of cycles N_i the crack takes to grow from a_i to $a_i + \delta a$ is given by:

$$N_0 = \frac{\delta a}{F(\Delta K(a_i), R, \Delta K_{th}, K_c, \ldots)} \tag{2}$$

$\Delta K(c_i)$ can be calculated by an expression similar to Equation (1), to get the correspondent growth in the direction of the semi-axis c, δc_i, which is given by:

$$\delta c_i = N_i \cdot F(\Delta K_{rms}(c_i), R_{rms}, \Delta K_{th}, K_c, \ldots) \tag{3}$$

The numerical calculation process can now start the coupled interactions making $\Delta K(a_1) = \Delta K(a_i + \delta a)$ and calculating $N_1 = \delta a/F(\Delta K(a_1), R, \Delta K_{th}, K_c, \ldots)$, in order to get $\delta c_1 = N_1 \cdot F(\Delta K(c_1), R_{rms}, \Delta K_{th}, K_c, \ldots)$, where $c_1 = c_i + \delta c_i$, etc. The precision of the methodology can be adjusted by the value of δa.

The well-known Paris–Erdogan is chosen for the crack growth law, modified to consider crack closure effects and the existence of a threshold stress intensity factor (SIF) range, $\Delta \boldsymbol{K}_{th}$:

$$\frac{da}{dN} = C \cdot \left(\Delta K_{eff}^{m} - \Delta K_{th}^{m} \right) \tag{4}$$

where C and m are constants. The effective stress intensity factor range, ΔK_{eff}, considering crack closure (or opening) effects, is determined by the following expression:

$$\Delta K_{eff} = K_{\max} - \max\left(K_{op}, K_{\min} \right) \tag{5}$$

where K_{max} and K_{min} are the SIFs attributable to the maximum and minimum stress level for each load cycle; and K_{op} = SIF corresponding with the crack opening stress level for a given load cycle (Newman and Jr. 1984).

In aluminum welds, short crack effects can be more significant than for steel. For example (Castro, Meggiolaro et al. 2012) and (Kitagawa and Takahashi 1976) describe the crack size influence on the fatigue propagation of short and long cracks. The crack size influence on the propagation threshold of short fatigue cracks under pulsating loads $\Delta K_{th}(a, R = 0)$ can be satisfactorily modelled using the short crack characteristic size a_0 proposed by (El Haddad, Topper et al. 1979):

$$\Delta K = \Delta\sigma \sqrt{\pi (a + a_0)} \quad \text{where} \quad a_0 = \left(1/\pi \right)\left(\Delta K_0 / \Delta S_0 \right) \tag{6}$$

Using a_0, it is indeed possible to reproduce the expected limits $\Delta K_{th}(a \to \infty) = \Delta K_0$ and $\Delta\sigma(a \to 0) = \Delta S_0$.

Alternatively, from an operational point of view, the short crack problem can be probably more clearly modelled by letting the SIF range ΔK retain its original equation, while the threshold expression (under pulsating loads) is modified to become a function of the crack length a, namely $\Delta K_0(a)$, resulting in:

$$\Delta K(a) = \Delta K_0 \cdot \sqrt{a / (a + a_0)} \tag{7}$$

Following Bazant's (Bažant 1997) reasoning, a more general equation can be used introducing an adjustable parameter γ:

$$\Delta K(a) = \Delta K_0 \cdot \left[1 + \left(a_0 / a \right)^{\gamma/2} \right]^{-1/\gamma} \tag{8}$$

For practical purpose, $\gamma = 6$ (Castro, Meggiolaro et al. 2012).

5 INPUT DATA FOR PROBABILISTIC ANALYSIS

This section presents a review of measurements reported in the literature for the various parameters required to implement the fracture mechanics model described in the previous section. These parameters can be organized as geometry, loading, and material parameters, including those describing the crack closure phenomenon. Fatigue analysis is performed by integrating Equation (4) and ends when the crack moves to fracture mode. In this case, a failure criterion must also be defined.

The geometry parameters include the dimensions of the specimen and the initial crack size. As the data was collected for FSW butt joints, only the dimensions of the cross section width w and thickness t are required to describe their geometry. In the IIW Recommendations on fatigue life in conventional welding, a thickness effect correction is considered. A lognormal distribution is considered for thickness with mean μ = 6.04 mm and standard deviation $\hat{\sigma}$ = 4.44 mm. For the width a lognormal distribution is also considered with μ = 31.35 mm and $\hat{\sigma}$ = 27.87 mm.

The initial crack size also contributes to a lower or higher fatigue life. This initial crack is generated in internal flaws and defects for certain FSW processing conditions. For example, a discontinuous wavy surface can be present after welding when there is a natural oxide layer presents on butt surfaces, generating a kissing bond (insufficient mixing of matter), weak bond or root flaw (Dickerson and Przydatek 2003, Di, Yang et al. 2006, Zhou, Yang et al. 2006, Zhou, Yang et al. 2006, Zhou, Yang et al. 2006, Li, Shen et al. 2011). Zhou et al. (Zhou, Yang et al. 2006) have already shown, for instance, that the fatigue life of flawed welds can be on the order of 33–80 times shorter than that of flaw-free welds. In this context, initial cracks and flaw were obtained from several authors from the literature (Dickerson and Przydatek 2003) (James, Hattingh et al. 2003) (Park, Kimura et al. 2004) (Baeslack Iii, Jata et al. 2006) (Zhang, Lin et al. 2006) (Ceschini, Boromei et al. 2007) (Di, Yang et al. 2007) (Chowdhury, Chen et al. 2010) (Vidal, Infante et al. 2010) (Li, Shen et al. 2011) (Sagar, Miyasaka et al. 2012) (Sharma, Dwivedi et al. 2012). A lognormal distribution with mean μ = 0.455 mm and standard deviation $\hat{\sigma}$ = 0.45 mm is considered.

In FSW butt joints, some authors (Bussu and Irving 2003, James, Hattingh et al. 2003, Zhou, Yang et al. 2005, Ali, An et al. 2007, Kainuma, Katsuki et al. 2008, Uematsu, Tokaji et al. 2009, Gemme, Verreman et al. 2011) have shown that the crack usually initiates on the surface or at the corner of the cross section. Therefore, for this analysis, two crack geometries are considered: (1) surface semi-elliptical, and (2) corner quart-elliptical. The ellipse is defined by semi-axis dimensions, a and c. In this work, the initial crack is assumed to be circular ($a_0 = c_0$).

The loading in fatigue tests is normally sufficiently controlled so as to be treated deterministically in a probabilistic fatigue analysis. However, the local residual stresses are often modelled probabilistically, due to their high variability. Recently, Kumar et al. (Kumar, Mishra et al. 2013) published a book discussing residual stresses in FSW joints, which describes the fundamentals of residual stresses and reviews the data reported for various materials. Several parameters affect mechanical properties, including residual stress levels. Kumar et al. (Kumar, Mishra et al. 2013) identify the following main parameters: tool transverse speed, tool rotation rate, and sample size. In addition, Deplus et al. (Deplus, Simar et al. 2011) reviewed some residual stress measures from the literature, and found values of the maximum tensile residual stress lower than those generated during fusion welding. For example, James and Mahoney (James and Mahoney) measured residual stress in the FSW 7050Al-T7451, C458 Al–Li alloy, and 2219Al by means of X-ray diffraction. The investigation showed that generally, longitudinal (parallel to welding direction) residual stresses were tensile and transverse (normal to welding direction) residual stresses were compressive. The low residual stress in the FSW welds was attributed to the lower heat input during FSW and the accommodation of stresses during recrystallization.

In the FSW tests, only the transverse residual stress (with respect to the weld direction) has a significant influence on fatigue behavior. While the residual stress distribution through the thickness is normally self-equilibrating, most of the fatigue life is spent during near surface small crack growth, so the residual stress at the surface is the most important from the point of view of fatigue behavior. Although Mahoney (James and Mahoney) found compressive stresses, the data obtained in this work show that they can be tensile and compressive (Ma, Staron et al. 2011) (John, Jata et al. 2003) (Hong, Kim et al. 2006) (Kuwayama, Asakawa et al. 2009) (Lemmen, Alderliesten et al. 2011) (Ma, Staron et al. 2011) (Lakshminarayanan and Balasubramanian 2012). Results were fitted by a normal distribution with μ = 8.45 MPa and $\hat{\sigma}$ = 17.95 MPa.

The welding of metals affects a number of parameters related to the fatigue crack growth behavior (ASTM 1990), including: the SIF threshold (ΔK_{th}), stress ratio (R), crack growth constants (C, m), failure mechanism, fracture toughness, etc. Mainly, these parameters are affected by the residual stress (Lee, Chung et al. 1998, Bussu and Irving 2003, John, Jata et al. 2003, Pasta and Reynolds 2008). In 2005, Mishra and Ma (Mishra and Ma 2005) did an extensive review of FSW, including the fatigue crack propagation behavior. They made the following observations: the quality of the FSW weld only exerted a limited effect on the da/dN–ΔK curve. At lower loads and R-ratios, the fatigue crack propagation properties of the FSW welds were superior to those of the base metal, due to compressive residual stresses present. At higher loads or R-radios, the effect of the compressive residual stress becomes less important and–similar to the base material–the specimen geometry becomes increasingly important. In addition, they discuss ΔK_{th} in FSW 2519Al and 7050Al alloys, where the values usually increase in the nugget and HAZ regions. Other similar results can be found in (Bussu and Irving 2003, John, Jata et al. 2003, Tra, Okazaki et al. 2012).

Fatigue crack growth in FSW joints also was extensively reviewed by Biro *et al.* (Biro, Chenelle et al. 2012). Using many sources, they show a direct relationship between residual stress and crack growth rate. In fact, the residual stress alters the effective R-ratio during cyclic testing. Since the transversal residual stress can be tensile or compressive the crack growth rate can decrease or increase in the weld when compared to the metal base (Moreira, de Jesus et al. 2008, Fratini, Pasta et al. 2009). This behavior can be explained by crack closure. Biro *et al.* (Biro, Chenelle et al. 2012) have moreover demonstrated crack path deviation in FSW joints. This deviation can be explained by different values of residual stress in the longitudinal and transverse directions, which affects the principal stresses around the crack tip (De Oliveira Miranda, Meggiolaro et al. 2003, Miranda, Meggiolaro et al. 2003).

Menzemer (Menzemer 1992) recommends that da/dN data obtained under constant K_{max} or high R-ratio conditions are used in conjunction with a crack growth law based on the effective SIF to consider residual stress effects. Kim et al. (Kim, Lee et al. 2008) have obtained da/dN results for 5083-H32 and 6061-T651 for R = 0.1 and R = 0.8. They considered a residual stress of -19±5 MPa at the crack tip. Biellas (Biallas 2013) reproduced results for 6063-T6 for R = 0.1, 0.5, and 0.8. Tra et al. (Tra, Okazaki et al. 2012) and Biallas (Biallas 2013) report value of $\Delta K_{th} \approx 1$ MPa$\sqrt{\text{m}}$.

The two curves, upper bound and *lower* bound were adjusted with the available experimental results with R = 0.8. They have the same value for exponent m = 4, but different values to C and ΔK_{th}, in the Paris-Erdogan equation. The upper and lower bound curves were plotted with LN(C) = -23.54 and -24.41, respectively, where C is in m/cycle. These values are used here to determine a probabilistic distribution for C as two values for 10% and 90% of probability in a cumulative distribution function. Considering a normal distribution, this approach results in μ = -23.97 and $\hat{\sigma}$ = 0.3 for LN(C) assuming units of MPa and m. The distribution of ΔK_{th} was adjusted with available data from Tra et al. (Tra, Okazaki et al. 2012) and Biallas (Biallas 2013), giving μ = 2.77 and $\hat{\sigma}$ = 0.56.

6 PROBABILISTIC SIMULATION ANALYSIS AND RESULTS

In this section, probabilistic simulation analyzes are performed using Monte Carlos simulation (MCS) and the results are compared with the S-N curves derived based on the previously presented statistical analysis of experimental data from the literature. MCS is described in a number of references (Ayyub 2003, Benaroya, Han et al. 2005, Kroese, Taimre et al. 2013). In essence, this analysis method consists of evaluating a limit state function numerous times, each time with a different set of randomly selected values for each variable, z_i, in the deterministic model. The probability of failure can then be determined from the following expression:

$$p_f = \frac{n\left(G(z) \leq 0\right)}{N_t} \tag{9}$$

wherein N_t is the total number of repetitions or trials, and $n(G(\mathbf{z})\leq 0)$ is the number of trials for which the limit state was violated. Figure 15 shows the general idea of the MCS analysis.

At the beginning of each trial, Figure 3(a), a random number is selected for each statistical variable z_i. There are many implemented algorithms to generate the random input data to the analysis. It can be generated directly from the statistical distribution to create a set of number that obeys a specific distribution. For example, the C++ language (C++11) has already implemented in the <random> header a set of high level classes to produce random numbers using combinations of generators and distributions (Network 2015). Alternatively, the random number (uniformly distributed between zero and one) can be obtained using the inverse of the cumulative distribution function (CDF) of the statistical variable. There are many available codes (Acklam 2010) for this purpose. In this paper, this last approach was used with the Mersenne Twister pseudo-random generator (Matsumoto and Nishimura 1998) of 32-bit numbers with a state size of 19937 bits implemented in the C++ library.

The determinist fracture mechanics analysis, can be stopped based on any one of three criteria: (1) when the maximum stress intensity factor achieves the critical fracture toughness, K_C; (2) when the crack growth rate became too fast to be considering a problem of fracture instead a problem of fatigue; and (3) when the crack reaches a critical size compared to the dimensions of the component subjected to fatigue loading (either an arbitrary limit or a limit based on the component failure by cross section yielding). The first two criteria are missing in the literature for FSW joints, so they are not considered in the analysis. The size criterion is commonly adopted in the crack propagation analysis of welding structures (Walbridge and Nussbaumer 2007, Walbridge and Nussbaumer 2008, Ghahremani and Walbridge 2011). In this context, a critical size of a_c = 0.5·thickness or c_c = 0.5· thickness is applied.

Using the deterministic fracture mechanics model, MCS was performed using the statistical variables in Table 1, based on the previously discussed literature review.

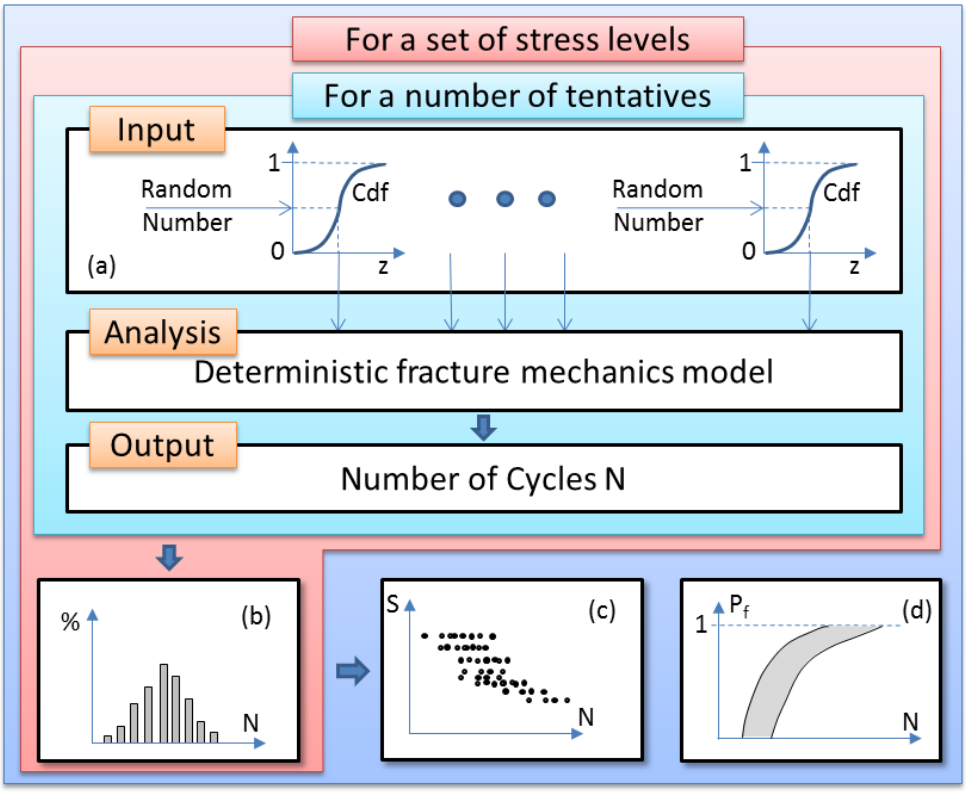

Figure 3 - General idea of probabilistic MCS analysis.

Table 1. Values of parameters for probabilistic MCS analysis

Parameter	Mean	Std. dev.	Distribution
Thickness (mm)	6.04	4.44	lognormal
Width (mm)	31.35	27.87	lognormal
a_{init} and c_{init} (mm)	0.45	0.45	lognormal
Residual Stress (MPa)	8.45	17.95	normal
m	4	-	uniform
LN (C)	-23.9	0.30	normal
ΔK_{th} (MPa√m)	2.77	0.56	lognormal
S_y (MPa)	152	36.88	lognormal
S_u (MPa)	243	60.16	lognormal
Vickers Hardness (HV)	78.0	13.51	lognormal

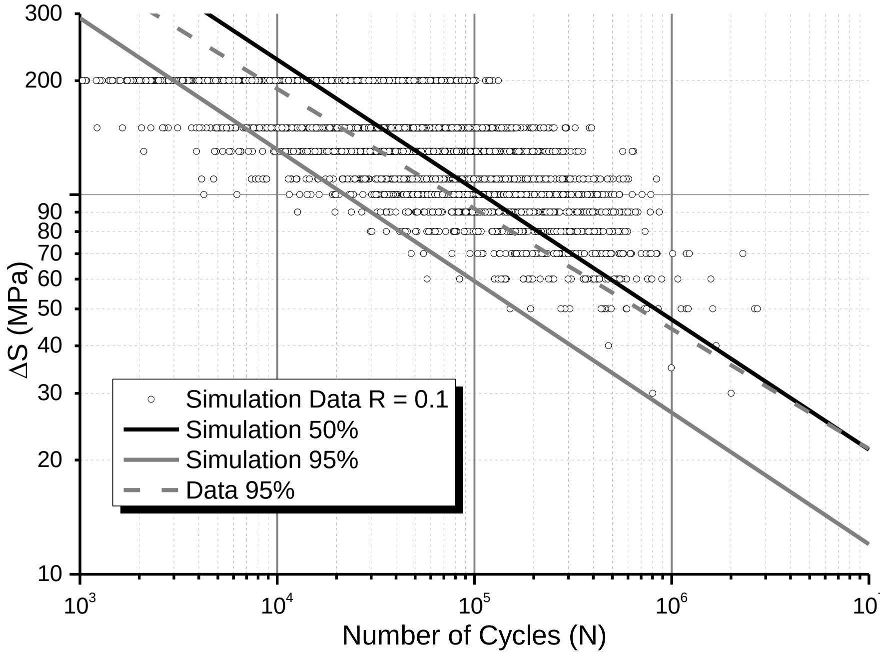

Figure 4. MCS results for *R* = 0.1 and 50% and 95% survival probability curves.

Figure 4 shows results of probabilistic analysis obtained by MCS for $R = 0.1$. Runouts are not shown – only simulations resulting in a finite life. Based on these results, 50% and 95% survival probability curves are plotted and compared with the 95% curve obtained earlier based on the collected fatigue test data. The curve based on the MCS simulations has m = 2.91 and $\Delta S(2{\cdot}10^6)$ = 21 MPa. This corresponds with a difference of 8% in the slope and 41% in the stress range $\Delta S(2{\cdot}10^6)$.

As recommend by Jaccard et al. (Jaccard, Kosteas et al. 1995), fixing the slope at m = 7.0 represents better the aluminum fatigue data for conventional welds, therefore, Figure 5 shows the 95% simulated survival probability curve, considering m = 7.0, with those presented previously: i.e. curves based on experimental and simulated data, with fixed and variable slope, for FSW and conventional welding. Note that the simulated curve with m = 7.0 lies between the FSW and conventional welding curves with $\Delta S(2{\cdot}10^6)$ = 53.6 MPa. Thus, the error in the reference stress range decreases to 13.5%.

Some strategies could be used to improve the MCS analysis to decrease the differences between the experimental data and simulation results. The simplest ones involve improving either the input data or the deterministic model. The deterministic model is an approximation of the mechanical behavior of crack propagation and it does not take into account: (a) the strain relief when the crack propagates in the cross section of the specimen; (b) the correct form of the crack front, which generally is generally not a perfect ellipse; and (c) the shape of initial crack size and shape. A more sophisticated determinist model should include these considerations. However a complete 3D finite element model, for example, can render MCS computationally unmanageable.

The weak input data in the analysis are believed to be the initial crack size and the crack growth properties of the material. The initial crack size was obtained from works that have reported it. However, many other works have not reported initial defect sizes. The initial crack size in conventional welds, for example, is about 0.10 – 0.15 mm with a lognormal distribution μ = 0.15 mm and $\hat{\sigma}$ = 0.045 mm (Coughlin and Walbridge 2011, Coughlin and Walbridge 2012). In addition, compared with conventional welds, the distribution of ΔK_{th} for

FSW is considered high (a lognormal distribution with μ = 0.94 MPa√m and $\hat{\sigma}$ = 0.19 MPa√m (Coughlin and Walbridge 2011, Coughlin and Walbridge 2012) is more typical). Both initial crack size and threshold have significant importance in the early crack propagation and where most of the total fatigue life is spent.

Considering the two distributions presented in the previous paragraph for conventional welds, two new MC analyses are performed to give an idea how these parameters can influence the results. Figure 6 shows these new results and Table 2 summarizes all of the results obtained in this work. The results show that curves can be obtained above and below the experimental design curve with small but reasonable modifications to these parameters. Also, they show the importance of obtaining more experimental data for initial defect size and crack growth rates with precision.

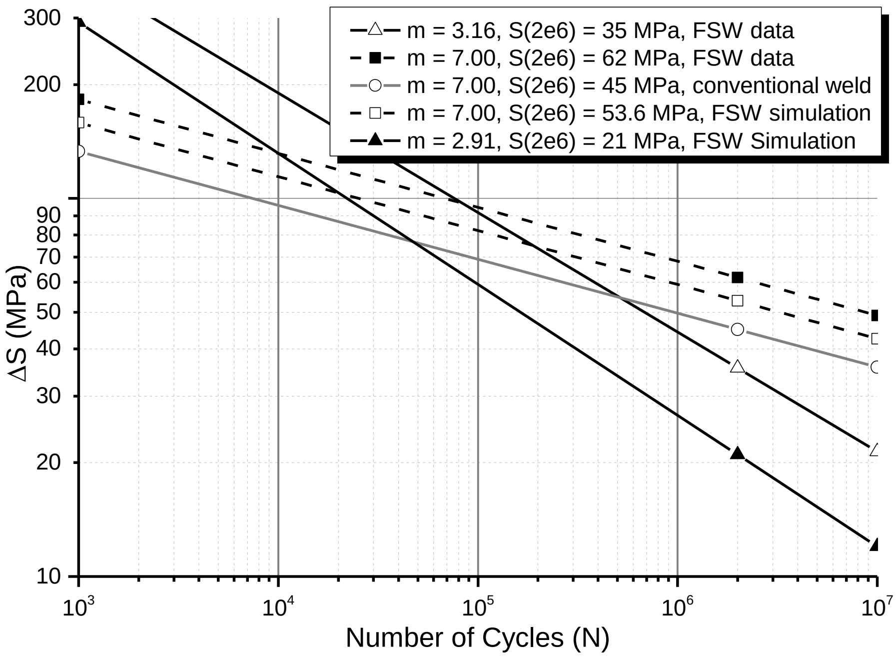

Figure 5. 95% survival probability curves for experimental and simulated data considering FSW and conventional welding

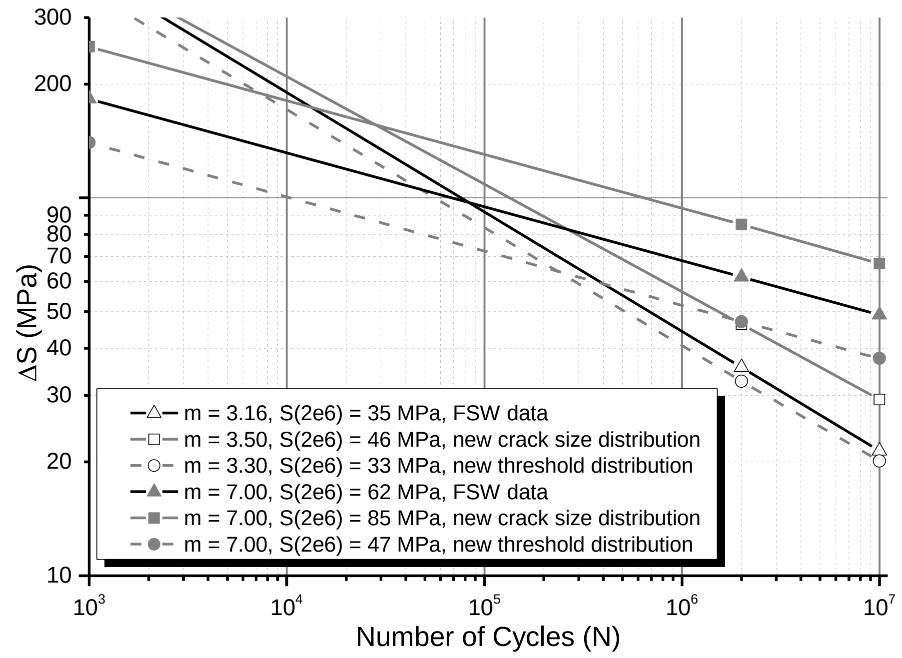

Figure 6. 95% survival probability curves for FSW based on experimental results and using various crack size and crack growth threshold assumptions

Table 2. Values SN parameters for experimental data and probabilistic simulations for 95% survival probability curves

Description	*m*	ΔS ($2{\cdot}10^6$) MPa	Difference %
FSW data	3.16	35.6	-
FSW simulation	2.91	21.0	-41.01
FSW simulation with new crack size distribution	3.50	46.0	29.21
FSW simulation with new threshold distribution	3.30	33.0	-7.30
FSW data	7.00	62.0	-
Conventional Weld data	7.00	45.0	-27.42
FSW simulation	7.00	53.6	-13.55
FSW simulation with new crack size distribution	7.00	85.0	37.10
FSW simulation with new threshold distribution	7.00	47.0	-24.19

7 SUMMARY AND CONCLUSIONS

The main results and conclusions of the work presented in this paper are as follows:

- Based on the analysis of test fatigue data for FSW butt joints under axial loading reported elsewhere in the literature, design curves are proposed for a survival probability of 95% or 97.7% with slope allowed to vary or fixed at m = 7.0. These curves are comparable with the existing curves in the IIW Recommendation and ADM for conventional welded butt joints.

- Statistical properties of input parameters for a fracture mechanics model are established through a similar review of the existing literature. Using statistical distributions established based on this review, it is demonstrated how a probabilistic fracture mechanics analysis can be performed to establish a similar set of survival probability curves.
- Further research is recommended to study the identified key input parameters, allowing further refinement of the probabilistic fracture mechanics analysis.

ACKNOWLEDGEMENTS

The first author would like to thank the National Council for Scientific and Technological Development (CNPq) for the financial support under post-doctorate program and University of Waterloo for providing the necessary space and resources used during the development of this work.

REFERENCES

Acklam, P. J. (2010). "An algorithm for computing the inverse normal cumulative distribution function." from http://home.online.no/~pjacklam/notes/invnorm/.

Ali, A., X. An, C. A. Rodopoulos, M. W. Brown, P. O'Hara, A. Levers and S. Gardiner (2007). "The effect of controlled shot peening on the fatigue behaviour of 2024-T3 aluminium friction stir welds." International Journal of Fatigue **29**(8): 1531-1545.

Anderson, T. L. (1994). Fracture Mechanics: Fundamentals and Applications, Second Edition, Taylor & Francis.

Association, A. (2010). Aluminum Design Manual: 2010, Aluminum Association, Incorporated.

ASTM (1990). Fatigue and Fracture Testing of Weldments, ASTM.

Ayyub, B. M. (2003). Risk Analysis in Engineering and Economics, CRC Press.

Baeslack Iii, W. A., K. V. Jata and T. J. Lienert (2006). "Structure, properties and fracture of friction stir welds in a high-temperature Al-8.5Fe-1.3V-1.7Si alloy (AA-8009)." Journal of Materials Science **41**(10): 2939-2951.

Bažant, Z. P. (1997). "Scaling of quasibrittle fracture: Asymptotic analysis." International Journal of Fracture **83**(1): 19-40.

Benaroya, H., S. M. Han and M. Nagurka (2005). Probability Models in Engineering and Science, Taylor & Francis.

Biallas, G. (2013). "Effect of welding residual stresses on fatigue crack growth thresholds." International Journal of Fatigue **50**: 10-17.

Biro, A. L., B. F. Chenelle and D. A. Lados (2012). "Processing, Microstructure, and Residual Stress Effects on Strength and Fatigue Crack Growth Properties in Friction Stir Welding: A Review." Metallurgical and Materials Transactions B: Process Metallurgy and Materials Processing Science: 1-16.

Bussu, G. and P. E. Irving (2003). "The role of residual stress and heat affected zone properties on fatigue crack propagation in friction stir welded 2024-T351 aluminium joints." International Journal of Fatigue **25**(1): 77-88.

Castro, J. T. P. D., M. A. Meggiolaro, A. C. D. O. Miranda, H. Wu, A. Imad and N. Benseddiq (2012). "Prediction of fatigue crack initiation lives at elongated notch roots using short crack concepts." International Journal of Fatigue **42**: 172-182.

Cavaliere, P., G. Campanile, F. Panella and A. Squillace (2006). "Effect of welding parameters on mechanical and microstructural properties of AA6056 joints produced by Friction Stir Welding." Journal of Materials Processing Technology **180**(1-3): 263-270.
Cavaliere, P., A. De Santis, F. Panella and A. Squillace (2009). "Effect of welding parameters on mechanical and microstructural properties of dissimilar AA6082-AA2024 joints produced by friction stir welding." Materials and Design **30**(3): 609-616.
Cavaliere, P., A. Squillace and F. Panella (2008). "Effect of welding parameters on mechanical and microstructural properties of AA6082 joints produced by friction stir welding." Journal of Materials Processing Technology **200**(1-3): 364-372.
Ceschini, L., I. Boromei, G. Minak, A. Morri and F. Tarterini (2007). "Effect of friction stir welding on microstructure, tensile and fatigue properties of the AA7005/10 vol.%Al2O3p composite." Composites Science and Technology **67**(3-4): 605-615.
Chowdhury, S. M., D. L. Chen, S. D. Bhole, X. Cao, E. Powidajko, D. C. Weckman and Y. Zhou (2010). "Tensile properties and strain-hardening behavior of double-sided arc welded and friction stir welded AZ31B magnesium alloy." Materials Science and Engineering A **527**(12): 2951-2961.
Coughlin, R. and S. Walbridge (2011). "Fatigue correction factors for welded aluminum highway structures." Canadian Journal of Civil Engineering **38**(10): 1082-1091.
Coughlin, R. and S. Walbridge (2012). "Fatigue testing and analysis of aluminum welds under in-service highway bridge loading conditions." Journal of Bridge Engineering **17**(3): 409-419.
Czechowski, M. (2005). "Low-cycle fatigue of friction stir welded Al-Mg alloys." Journal of Materials Processing Technology **164-165**: 1001-1006.
Das, H., D. Chakraborty and T. Kumar Pal (2014). "High-cycle fatigue behavior of friction stir butt welded 6061 aluminium alloy." Transactions of Nonferrous Metals Society of China (English Edition) **24**(3): 648-656.
De Castro, J. T. P., A. Giassone and P. P. Kenedi (1998). "Fatigue Propagation of Superficial Semi and Quart-Elliptical Cracks in Wet Welds." Revista Brasileira de Ciencias Mecanicas/Journal of the Brazilian Society of Mechanical Sciences **20**(2): 263-277.
De Oliveira Miranda, A. C., M. A. Meggiolaro, J. T. P. De Castro and L. F. Martha (2003). "Fatigue life prediction of complex 2D components under mixed-mode variable amplitude loading." International Journal of Fatigue **25**(9-11): 1157-1167.
Deplus, K., A. Simar, W. Haver and B. Meester (2011). "Residual stresses in aluminium alloy friction stir welds." The International Journal of Advanced Manufacturing Technology **56**(5-8): 493-504.
Di, S., X. Yang, D. Fang and G. Luan (2007). "The influence of zigzag-curve defect on the fatigue properties of friction stir welds in 7075-T6 Al alloy." Materials Chemistry and Physics **104**(2–3): 244-248.
Di, S., X. Yang, G. Luan and B. Jian (2006). "Comparative study on fatigue properties between AA2024-T4 friction stir welds and base materials." Materials Science and Engineering: A **435–436**(0): 389-395.
Dickerson, T. L. and J. Przydatek (2003). "Fatigue of friction stir welds in aluminium alloys that contain root flaws." International Journal of Fatigue **25**(12): 1399-1409.
El Haddad, M. H., T. H. Topper and K. N. Smith (1979). "Prediction of non propagating cracks." Engineering Fracture Mechanics **11**(3): 573-584.
Ericsson, M., L. Z. Jin and R. Sandström (2007). "Fatigue properties of friction stir overlap welds." International Journal of Fatigue **29**(1): 57-68.
Ericsson, M. and R. Sandström (2003). "Influence of welding speed on the fatigue of friction stir welds, and comparison with MIG and TIG." International Journal of Fatigue **25**(12): 1379-1387.

Fratini, L., S. Pasta and A. P. Reynolds (2009). "Fatigue crack growth in 2024-T351 friction stir welded joints: Longitudinal residual stress and microstructural effects." International Journal of Fatigue **31**(3): 495-500.

Gemme, F., Y. Verreman, L. Dubourg and P. Wanjara (2011). "Effect of welding parameters on microstructure and mechanical properties of AA7075-T6 friction stir welded joints." Fatigue and Fracture of Engineering Materials and Structures **34**(11): 877-886.

Ghahremani, K. and S. Walbridge (2011). "Fatigue testing and analysis of peened highway bridge welds under in-service variable amplitude loading conditions." International Journal of Fatigue **33**(3): 300-312.

Grujicic, M., G. Arakere, B. Panduragan, A. Hariharan, C. F. Yen, B. A. Cheeseman and C. Fountzoulas (2011). "Statistical analysis of high-cycle fatigue behavior of friction stir welded AA5083-H321." Journal of Materials Engineering and Performance **20**(6): 855-864.

Hagisawa, N. and I. Okura (2009). "Influence of stress ratios on fatigue strength of A6005C-T5 aluminum alloy and its friction stir welded joints." Doboku Gakkai Ronbunshuu A **65**(1): 117-122.

Hattel, J. H., M. R. Sonne and C. C. Tutum (2014). "Modelling residual stresses in friction stir welding of Al alloys—a review of possibilities and future trends." International Journal of Advanced Manufacturing Technology.

He, X., F. Gu and A. Ball (2014). "A review of numerical analysis of friction stir welding." Progress in Materials Science **65**: 1-66.

Hobbacher, A. (2007). Recommendations for Fatigue Design of Welded Joints and Components. XIII-2151-07/XV-1254-07, International Institute of Welding.

Hong, S., S. Kim, C. G. Lee and S. J. Kim (2006). "Fatigue crack propagation behavior of friction stir welded Al-Mg-Si alloy." Scripta Materialia **55**(11): 1007-1010.

Jaccard, R., D. Kosteas and R. Ondra (1995). Backgroud document to fatigue design curves for welded aluminium components. IIW Doc. No.XIII-1588-95. IIW Doc. No.XIII-1588-95.

James, M. and M. Mahoney Residual stress measurements in friction stir welded aluminium alloys. First International Symposium on Friction Stir Welding, Thousand Oaks, CA, USA.

James, M. N., G. R. Bradley, H. Lombard and D. G. Hattingh (2005). "The relationship between process mechanisms and crack paths in friction stir welded 5083-H321 and 5383-H321 aluminium alloys." Fatigue and Fracture of Engineering Materials and Structures **28**(1-2): 245-256.

James, M. N., D. G. Hattingh and G. R. Bradley (2003). "Weld tool travel speed effects on fatigue life of friction stir welds in 5083 aluminium." International Journal of Fatigue **25**(12): 1389-1398.

John, R., K. V. Jata and K. Sadananda (2003). "Residual stress effects on near-threshold fatigue crack growth in friction stir welds in aerospace alloys." International Journal of Fatigue **25**(9-11): 939-948.

Kainuma, S., H. Katsuki, I. Iwai and M. Kumagai (2008). "Evaluation of fatigue strength of friction stir butt-welded aluminum alloy joints inclined to applied cyclic stress." International Journal of Fatigue **30**(5): 870-876.

Kim, S., C. G. Lee and S. J. Kim (2008). "Fatigue crack propagation behavior of friction stir welded 5083-H32 and 6061-T651 aluminum alloys." Materials Science and Engineering A **478**(1-2): 56-64.

Kitagawa, H. and S. Takahashi (1976). Applicability of fracture mechanics to very small crack or cracks in the early stage. 2nd international conference on mechanical behavior of materials, ASM.

Kobayashi, Y., M. Sakuma, Y. Tanaka and K. Matsuoka (2007). "Fatigue strength of friction stir welding joints of aluminium alloy 6082 extruded shape." Welding International **21**(1): 18-24.

Kroese, D. P., T. Taimre and Z. I. Botev (2013). Handbook of Monte Carlo Methods, Wiley.

Kumar, N., R. S. Mishra and J. A. Baumann (2013). Residual Stresses in Friction Stir Welding: A volume in the Friction Stir Welding and Processing Book Series, Elsevier Science.

Kuwayama, K., M. Asakawa, T. Okada, T. Nakamura, S. Machida and S. Fujita (2009). Fatigue crack propagation property of friction stir welded 2024-T3 aluminum alloy. Collection of Technical Papers - AIAA/ASME/ASCE/AHS/ASC Structures, Structural Dynamics and Materials Conference.

Lakshminarayanan, A. K. and V. Balasubramanian (2012). "Assessment of fatigue life and crack growth resistance of friction stir welded AISI 409M ferritic stainless steel joints." Materials Science and Engineering A **539**: 143-153.

Lee, Y. B., C. S. Chung, Y. K. Park and H. K. Kim (1998). "Effects of redistributing residual stress on the fatigue behavior of SS330 weldment." International Journal of Fatigue **20**(8): 565-573.

Lemmen, H. J. K., R. C. Alderliesten and R. Benedictus (2011). "Evaluating the fatigue initiation location in friction stir welded AA2024-T3 joints." International Journal of Fatigue **33**(3): 466-476.

Li, B., Y. Shen and W. Hu (2011). "The study on defects in aluminum 2219-T6 thick butt friction stir welds with the application of multiple non-destructive testing methods." Materials and Design **32**(4): 2073-2084.

Ma, Y. E., P. Staron, T. Fischer and P. E. Irving (2011). "Size effects on residual stress and fatigue crack growth in friction stir welded 2195-T8 aluminium - Part I: Experiments." International Journal of Fatigue **33**(11): 1417-1425.

Ma, Y. E., P. Staron, T. Fischer and P. E. Irving (2011). "Size effects on residual stress and fatigue crack growth in friction stir welded 2195-T8 aluminium – Part II: Modelling." International Journal of Fatigue **33**(11): 1426-1434.

Ma, Z. Y. (2008). "Friction stir processing technology: A review." Metallurgical and Materials Transactions A: Physical Metallurgy and Materials Science **39 A**(3): 642-658.

Maddox, S. J. (2003). "Review of fatigue assessment procedures for welded aluminium structures." International Journal of Fatigue **25**(12): 1359-1378.

Mahdavi Shahri, M., T. Höglund and R. Sandström (2012). "Eurocode 9 to estimate the fatigue life of friction stir welded aluminium panels." Engineering Structures **45**(0): 307-313.

Matsumoto, M. and T. Nishimura (1998). "Mersenne twister: a 623-dimensionally equidistributed uniform pseudo-random number generator." ACM Trans. Model. Comput. Simul. **8**(1): 3-30.

Matsuoka, K. and S. Kitamura (1999). "Proof strength of aluminium alloy 6N01-T5 extrusion butt welded joint." Keikinzoku Yosetsu/Journal of Light Metal Welding and Construction **37**(5): 1-10.

Menzemer, C. C. (1992). Fatigue behavior of welded aluminum structures.

Miranda, A. C. O., M. A. Meggiolaro, J. T. P. Castro, L. F. Martha and T. N. Bittencourt (2003). "Fatigue life and crack path predictions in generic 2D structural components." Engineering Fracture Mechanics **70**(10): 1259-1279.

Mishra, R. S. and Z. Y. Ma (2005). "Friction stir welding and processing." Materials Science and Engineering: R: Reports **50**(1–2): 1-78.

Moreira, P. M. G. P., M. A. V. de Figueiredo and P. M. S. T. de Castro (2007). "Fatigue behaviour of FSW and MIG weldments for two aluminium alloys." Theoretical and Applied Fracture Mechanics **48**(2): 169-177.

Moreira, P. M. G. P., A. M. P. de Jesus, A. S. Ribeiro and P. M. S. T. de Castro (2008). "Fatigue crack growth in friction stir welds of 6082-T6 and 6061-T6 aluminium alloys: A comparison." Theoretical and Applied Fracture Mechanics **50**(2): 81-91.

Murr, L. E. (2010). "A review of FSW research on dissimilar metal and alloy systems." Journal of Materials Engineering and Performance **19**(8): 1071-1089.

Nandan, R., T. DebRoy and H. K. D. H. Bhadeshia (2008). "Recent advances in friction-stir welding - Process, weldment structure and properties." Progress in Materials Science **53**(6): 980-1023.

Neto, D. M. and P. Neto (2013). "Numerical modeling of friction stir welding process: A literature review." International Journal of Advanced Manufacturing Technology **65**(1-4): 115-126.

Network, T. C. R. (2015). "cplusplus.com." from http://www.cplusplus.com/.

Newman, J. C. and Jr. (1984). "A crack opening stress equation for fatigue crack growth." International Journal of Fracture **24**(4): R131-R135.

Newman Jr, J. C. (1979). "REVIEW AND ASSESSMENT OF THE STRESS-INTENSITY FACTORS FOR SURFACE CRACKS." ASTM Special Technical Publication: 16-46.

Okura, I., N. Hagisawa, M. Naruo and H. Toda (2003). "Fatigue behavior of aluminum deck fabricated by friction stir welding." Structural Engineering/Earthquake Engineering **20**(1): 55s-67s.

Park, H. S., T. Kimura, T. Murakami, Y. Nagano, K. Nakata and M. Ushio (2004). "Microstructures and mechanical properties of friction stir welds of 60% Cu-40% Zn copper alloy." Materials Science and Engineering A **371**(1-2): 160-169.

Pasta, S. and A. P. Reynolds (2008). "Residual stress effects on fatigue crack growth in a Ti-6Al-4V friction stir weld." Fatigue and Fracture of Engineering Materials and Structures **31**(7): 569-580.

Rai, R., A. De, H. K. D. H. Bhadeshia and T. DebRoy (2011). "Review: Friction stir welding tools." Science and Technology of Welding and Joining **16**(4): 325-342.

Raju, I. S. and J. C. Newman (1988). Stress-Intensity Factors for Corner Cracks in Rectangular Bars. Fracture Mechanics, Nineteenth Symposium, Edição 969. T. A. Cruse**:** 43-55.

Sagar, S. P., C. Miyasaka, M. Ghosh and B. R. Tittmann (2012). "NDE of friction stir welds of Al alloys using high-frequency acoustic microscopy." Nondestructive Testing and Evaluation **27**(4): 375-389.

Sano, Y., K. Masaki, T. Gushi and T. Sano (2012). "Improvement in fatigue performance of friction stir welded A6061-T6 aluminum alloy by laser peening without coating." Materials and Design **36**: 809-814.

Scialpi, A., M. De Giorgi, L. A. C. De Filippis, R. Nobile and F. W. Panella (2008). "Mechanical analysis of ultra-thin friction stir welding joined sheets with dissimilar and similar materials." Materials and Design **29**(5): 928-936.

Sharma, C., D. K. Dwivedi and P. Kumar (2012). "Effect of welding parameters on microstructure and mechanical properties of friction stir welded joints of AA7039 aluminum alloy." Materials and Design **36**: 379-390.

Shtrikman, M. M. (2008). "Current state and development of friction stir welding Part 3. Industrial application of friction stir welding." Welding International **22**(11): 806-815.

Standardization, E. C. f. (2007). Eurocode 9: Design of aluminium structures - Part 1-3: Structures susceptible to fatigue.

Standardization, I. O. f. (2011). Friction stir welding — Aluminium, International Organization for Standardization.
Tra, T. H., M. Okazaki and K. Suzuki (2012). "Fatigue crack propagation behavior in friction stir welding of AA6063-T5: Roles of residual stress and microstructure." International Journal of Fatigue **43**: 23-29.
Uematsu, Y., K. Tokaji, H. Shibata, Y. Tozaki and T. Ohmune (2009). "Fatigue behaviour of friction stir welds without neither welding flash nor flaw in several aluminium alloys." International Journal of Fatigue **31**(10): 1443-1453.
Uematsu, Y., K. Tokaji, Y. Tozaki and H. Shibata (2006). "Fatigue behavior of friction stir welded joints of 6061-T6 aluminum alloy." Zairyo/Journal of the Society of Materials Science, Japan **55**(1): 49-54.
Uzun, H., C. Dalle Donne, A. Argagnotto, T. Ghidini and C. Gambaro (2005). "Friction stir welding of dissimilar Al 6013-T4 To X5CrNi18-10 stainless steel." Materials and Design **26**(1): 41-46.
Vidal, C., V. Infante and P. Vilaa (2010). Assessment of improvement techniques effect on fatigue behaviour of friction stir welded aerospace aluminium alloys. Procedia Engineering.
Vidal, C., V. Infante and P. Vilaça (2014). "Fatigue behaviour at elevated temperature of friction stir channelling solid plates of AA5083-H111 aluminium alloy." International Journal of Fatigue **62**: 85-92.
Vigh, L. G. and I. Okura (2013). "Fatigue behaviour of Friction Stir Welded aluminium bridge deck segment." Materials & Design **44**(0): 119-127.
Walbridge, S. and A. Nussbaumer (2007). "A probabilistic model for determining the effect of post-weld treatment on the fatigue performance of tubular bridge joints." International Journal of Fatigue **29**(3): 516-532.
Walbridge, S. and A. Nussbaumer (2008). "A probabilistic assessment of the effect of post-weld treatment on the fatigue performance of tubular truss bridges." Engineering Structures **30**(1): 247-257.
Zhang, H., S. B. Lin, L. Wu, J. C. Feng and S. L. Ma (2006). "Defects formation procedure and mathematic model for defect free friction stir welding of magnesium alloy." Materials and Design **27**(9): 805-809.
Zhou, C., X. Yang and G. Luan (2005). "Fatigue properties of friction stir welds in Al 5083 alloy." Scripta Materialia **53**(10): 1187-1191.
Zhou, C., X. Yang and G. Luan (2006). "Effect of kissing bond on fatigue behavior of friction stir welds on Al 5083 alloy." Journal of Materials Science **41**(10): 2771-2777.
Zhou, C., X. Yang and G. Luan (2006). "Effect of oxide array on the fatigue property of friction stir welds." Scripta Materialia **54**(8): 1515-1520.
Zhou, C., X. Yang and G. Luan (2006). "Effect of root flaws on the fatigue property of friction stir welds in 2024-T3 aluminum alloys." Materials Science and Engineering A **418**(1-2): 155-160.
Zhou, C., X. Yang and G. Luan (2006). "Investigation of microstructures and fatigue properties of friction stir welded Al-Mg alloy." Materials Chemistry and Physics **98**(2-3): 285-290.